2,3 Butanedione Monoxime Affects CFTR Channel Function Through Phosphorylation-Dependent and Phosphorylation-Independent Mechanisms. The role of bilayer material properties.

Pablo Artigas, Subhi J. Al'Aref, E. Ashley Hobart, Laín F. Díaz

Masayuki Sakaguchi, Samuel Straw and Olaf S. Andersen.

Laboratory of Cardiac/Membrane Physiology, The Rockefeller University, New York, NY 10021. (P.A., L.F.D., M.S., S.S.)

Department of Physiology and Biophysics, Weill Medical College of Cornell University, New York, New York, 10021. (S.J.A., E.A.H., O.S.A.)

Instituto de Ciencias Biomédicas and Centro de Estudios Moleculares de la Célula, Facultad de Medicina, Universidad de Chile, Santiago, Chile (L.F.D.)

Running title: BDM alters CFTR gating and bilayer properties

Corresponding author:

Pablo Artigas

Laboratory of Cardiac/Membrane Physiology

The Rockefeller University

1230 York Avenue, 10021

New York, NY

Telephone: 212-3278617

Fax: 212-3277589

email: artigas@rockefeller.edu

Abbreviations: BDM, 2,3 butanedione monoxime; CFTR, cystic fibrosis transmembrane conductance regulator; PKA, cAMP-dependent protein kinase; PKI, PKA peptide inhibitor; PP, protein phosphatase; DOPC, dioleoylphosphatidylcholine

ABSTRACT

2,3-butanedione monoxime (BDM) is widely believed to act as a chemical phosphatase. We therefore examined BDM's effects on the cystic fibrosis transmembrane conductance regulator (CFTR) Cl^- channel, which is regulated by phosphorylation in a complex manner. In guinea pig ventricular myocytes, forskolin-activated whole-cell CFTR currents responded biphasically to external 20 mM BDM: a rapid ~2-fold current activation was followed by a slower (τ ~20 s) inhibition (to ~20 % of control). The inhibitory response was abolished by intracellular dialysis with the phosphatase inhibitor microcystin, suggesting involvement of endogenous phosphatases. The BDM-induced activation was studied further in *Xenopus* oocytes expressing human epithelial CFTR. The concentration for half-maximal BDM activation ($K_{0.5}$) was state-dependent, ~2 mM for highly and ~20 mM for partially phosphorylated channels, suggesting a modulated receptor mechanism. Because BDM modulates many different membrane proteins with similar $K_{0.5}$s, we tested whether BDM could alter protein function by altering lipid bilayer properties rather than by direct BDM-protein interactions. Using gramicidin channels of different lengths (different channel-bilayer hydrophobic mismatch) as reporters of bilayer stiffness, we found that BDM increases channel appearance rates and lifetimes (reduces bilayer stiffness). At 20 mM BDM, the appearance rates increase ~4 fold (for the longer, 15 residues/monomer, channels) to ~10 fold (for the shorter, 13 residues/monomer, channels); the lifetimes increase ~50% independent of channel length. BDM thus reduces the energetic cost of bilayer deformation, an effect that may underlie BDM's effects on CFTR and other membrane proteins; the state-dependent changes in $K_{0.5}$ are consistent with such a bilayer-mediated mechanism.

INTRODUCTION

The oxime, 2,3-Butanedione monoxime (BDM), is a myosin ATPase inhibitor (Higuchi and
Takemori, 1989) widely used as a research tool in cell biology (Titus, 2003). BDM is an
inhibitor of muscle contraction (e.g. Baker et al, 2004), which may have clinical use in heart
transplantation (Warnecke et al, 2002), but the cellular targets of BDM remain elusive (Titus,
2003). Previously BDM was used as a brain-barrier permeant reactivator of organophosphorous-
inhibited acetylcholinesterase, and it has been proposed to act as a "chemical phosphatase"
removing phosphate groups by nucleophilic attack (Holmstedt, 1959). Consistent with such an
effect, BDM promotes dephosphorylation in ventricular myocytes (Wiggins et al, 1980) and
some reports indicate that its effects on several channels, in different cell types, are antagonized
by phosphorylation (Sellin and McArdle, 1994). But BDM affects many ion channels and
transporters without changing their phosphorylation (e.g. Lopatin and Nichols, 1993; Watanabe
et al, 2001) suggesting "direct" BDM-protein interaction.

The cystic fibrosis transmembrane conductance regulator (CFTR) is a Cl^- channel whose
activation requires phosphorylation by cAMP-dependent protein kinase (PKA); its activity is
regulated by phosphorylation at several serine residues in its regulatory (R) domain (reviewed by
Gadsby and Nairn, 1999). We tested the actions of BDM on CFTR currents (I_{CFTR}), expecting a
current reduction due to BDM's putative phosphatase activity. Surprisingly, BDM induced
complex responses – including both activation and inhibition of I_{CFTR} – depending on the
condition of drug administration. These opposite effects of BDM reflect different mechanisms;
only the inhibitory effect is likely to result from channel dephosphorylation.

The BDM-induced enhancement of I_{CFTR} shows similarities to the effects of genistein (Weinreich
et al, 1997) and capsaicin (Ai et al, 2004). Like BDM, these drugs alter the function of many
membrane proteins (Table 1, in Discussion), possibly reflecting their ability to alter lipid bilayer

properties rather than direct binding to their apparent target proteins (Hwang et al, 2003;

Lundbæk et al, 2005).

Lipid bilayers are elastic bodies (Evans and Hochmuth, 1978), and membrane proteins undergo

conformational changes that involve the protein/bilayer boundary (Lee, 2003). The hydrophobic

coupling between membrane proteins and the lipid bilayer therefore means that protein

conformational changes that perturb the local bilayer packing (Fig. 1) will incur an energetic cost

(Mouritsen and Bloom, 1984) — and protein function should, in principle, be regulated by

changes in bilayer material properties (Sackmann, 1984; Gruner, 1991), e.g. the changes in

monolayer intrinsic curvature (e.g. Gruner, 1985) and elastic moduli (Evans et al., 1995; Ly and

Longo, 2004) caused by the adsorption of amphiphiles. Such pharmacologically induced

changes in bilayer properties indeed can alter membrane protein function (Lundbæk et al., 2004;

Lundbæk et al. 2005). Could the widespread effects of BDM on membrane protein function

result from similar changes in bilayer properties?

To address this question, we used gramicidin (gA) channels as molecular force transducers

(Andersen et al., 1999) to monitor whether BDM induces changes in bilayer properties.

Gramicidin channels are formed by trans-bilayer association of two monomers:

(Scheme I)

where M denotes the non-conducting monomers, D the conducting dimers, and k_1 and k_{-1} the rate

constants for channel formation and dissociation. When the bilayer's hydrophobic thickness, d_0

(the distance between the carbonyl carbons in the two leaflets, Fig. 1), is larger than the

channel's hydrophobic length, l (length of the protein region containing highly hydrophobic

residues, Fig. 1), the bilayer thickness will adjust locally to match the channel length (cf. Fig. 1).

This bilayer deformation incurs an energetic cost, ΔG_{def}^0, which varies with bilayer thickness,

intrinsic monolayer curvature, c_0, which denotes the membrane lipids' propensity to form curved

(or non-bilayer) structures, and bilayer elastic moduli (Huang, 1986; Nielsen and Andersen, 2000; Lundbæk et al., 2005):

$$\Delta G_{def}^0 = H_B \cdot (d_0 - l)^2 + H_X \cdot (d_0 - l) \cdot c_0 + H_C \cdot c_0^2, \qquad (1)$$

where the coefficients H_B, H_X and H_C are functions of the bilayer elastic moduli, the bilayer thickness and the protein radius. ΔG_{def}^0 contributes to the overall free energy of gramicidin channel formation: ΔG_{tot}^0 ($= \Delta G_{prot}^0 + \Delta G_{def}^0$, where ΔG_{prot}^0 denotes the free energy change of the dimerization *per se*, excluding the interactions with the bilayer). Because ΔG_{def}^0 varies as a function of the hydrophobic mismatch ($d_0 - l$), the bilayer will respond to the deformation by imposing a disjoining force on the channels. Changes in this disjoining force will be observable as changes in the channel appearance rate and lifetime. Operationally, we describe changes in bilayer properties that, at a constant bilayer thickness, alter the disjoining force as changes in *bilayer stiffness* (Lundbæk et al., 2005). A decrease in stiffness will decrease the disjoining force and increase gramicidin channel appearance rate and lifetime and *vice versa*.

Indeed, gramicidin channels formation rate, and their lifetime, increase at concentrations where BDM affects the activity of CFTR and many other BDM-sensitive membrane proteins. More detailed analysis shows that BDM's promiscuous phosphorylation-independent actions may reflect its modification of the bilayer deformation energy rather than BDM-protein interaction.

MATERIALS and METHODS

CFTR experiments

<u>*Ventricular myocytes*</u>   The procedures for isolation and storage of Guinea pig ventricular myocytes were described previously (Hwang et al, 1993). All patch-clamp experiments were done using an AxoPatch 200B, a Digidata 1200 A/D board and pClamp (6 or 8) software (all from Axon instruments Inc). The results were stored on a personal computer and also continuously acquired on VCR tapes using a Neurocorder 384 (Neurodata Instruments Co.).

Whole-cell recordings were done at ~36 °C, using wide-tipped (0.8-1.5 MΩ) borosilicate glass (PG52151–4; WPI) pipettes with an intrapipette perfusion device inserted as described (Hwang et al, 1993). The pipette solution for intracellular dialysis contained (in mM): 85 aspartic acid, 5 pyruvic acid, 10 EGTA, 20 tetraethyl ammonium (TEA)-Cl, 2 $MgCl_2$, 5 $Tris_2$-creatine phosphate, 10 MgATP, 0.1 $Tris_{2.5}$-GTP, 10 HEPES, 5.5 glucose (buffered to pH 7.4 with CsOH). Myocytes were held at 0 mV and continuously superperfused with a solution containing (in mM): 145 NaCl, 1.5 $MgCl_2$, 1 $BaCl_2$, 0.5 $CdCl_2$, 5 HEPES, 5.5 glucose (pH 7.4 with NaOH). The time constant for exchange of the extracellular solution was ~4 s, depending on the position of the myocyte in the perfusion chamber.

Excised inside-out recordings were done at 22-23 °C with wide-tipped (14-18 μm diameter) borosilicate glass (N51A; Drummond Scientific) pipettes, coated with Sylgard to reduce noise and with a mineral oil/parafilm mixture to help gigaohm seal formation. Pipette resistance was 0.3-0.45 MΩ when filled with an extracellular solution containing (in mM): 145 N-methyl-D-glucamine (NMG)-Cl, 5 CsCl, 2 $BaCl_2$, 2.3 $MgCl_2$, 0.5 $CdCl_2$, 10 TES (pH 7.4). Patches were formed on membrane blebs (induced by exposing the myocytes to a hypotonic solution composed of (in mM) 67 KCl, 1.5 $MgCl_2$, 10 glucose, 10 HEPES, 2.5 EGTA (pH 7.0)), the patches held at 0 mV, excised, and transferred to a homemade flow chamber where the

intracellular face of the membrane was superfused continuously with a solution containing (in mM): 140 NMG-aspartate, 20 TEA-OH, 2 $MgCl_2$, 10 EGTA, 10 TES, (pH 7.4). Current was acquired at 1 kHz and filtered at 100 Hz.

Xenopus oocytes Oocytes were isolated enzymatically as described (Chan et al, 2000), injected with 0.05 ng of RNA encoding for human wild type epithelial CFTR and kept for 20-36 h at 18 °C until recording. Currents were recorded at room temperature, in a solution containing (in mM): 82.5 NaCl, 2 KCl, 1 $MgCl_2$, 5 HEPES (pH 7.4), using a voltage-clamp amplifier (OC-725A oocyte clamp; Warner Instrument Corp.). Signals were filtered at 1 kHz with an 8-pole Butterworth filter (Frequency Devices, Inc.) and acquired at 2 kHz using a Digidata 1200 A/D board and pClamp 6 software. A Minidigi 1A and Axoscope 9 (Axon Instruments) were used for continuous data acquisition at 10 Hz). When filled with 3M KCl, the resistance of the current microelectrode was 0.5–1 MΩ and that of the voltage electrode 1-2 MΩ.

Drugs: BDM was dissolved directly in the bath solutions. Forskolin and cantharidin (from Sigma) were added from 200 mM stock solutions in DMSO. Microcystin (from Calbiochem) was diluted in the pipette solution from a 10 mM solution in DMSO. The catalytic subunit of PKA and its peptide inhibitor PKI (generous gifts from Dr. Angus Nairn, Rockefeller University) were added to the bath or injected into oocytes, respectively, from aqueous stocks containing 1 mg/ml for PKA (MW 40kD) and 44 mg/ml for PKI (MW 2.2 kD). MgATP was added from a 200 mM stock in water (pH 7.4 with NMG).

Data analysis pClamp 9 and Origin 7 (OriginLab corp.) were used for analysis of current voltage (*I-V*) relationships and exponential decay of the whole-cell currents. For the single-channel recordings, currents from excised patches containing 2-4 channels were baseline subtracted, idealized and their open probability (P_O) calculated with programs kindly provided by

Lazlo Csanády (Csanády, 2000). The high P_O of cardiac CFTR (Gadsby and Nairn, 1999; see also Fig. 4 below) allowed counting the number of channels in the patch to estimate P_O. CFTR data are presented as average ± S.E.M.

Gramicidin experiments

The gramicidin analogue [Ala^1]gA (AgA(15)), its enantiomer [D-Ala^1]gA$^-$ (AgA$^-$(15)) and the sequence-shortened analogue des-(Val^1-Gly^2)-gA$^-$ (gA$^-$(13)), were generous gifts from Dr. Roger E. Koeppe II (University of Arkansas). They were synthesized and purified as described previously (Greathouse et al., 1999), and used as 1 − 10 nM solutions in ethanol.

Planar bilayers were formed from *n*-decane solutions (20 mg/ml) of dioleoylphosphatidylcholine (DOPC) from Avanti Polar Lipids (Alabaster, AL) across a hole (~1.6 mm diameter) in a Teflon® partition separating two aqueous solutions of 1.0 M NaCl (buffered to pH 7 with 10 mM HEPES). To minimize the loss of the hydrophobic BDM from the aqueous solution, the total volume of the lipid/decane solution used was less than 2 μL (or 1/1000-fold less than the volume of the aqueous solution). The applied potential was 200 mV. The gramicidins were added from ethanolic stock solutions to the electrolyte solution on either side of the bilayer; the BDM was added from DMSO stock solutions, again to both sides of the membrane. The final ethanol and DMSO concentrations were less than 0.5% (or 90 mM) and 0.4% (or 60 mM), respectively; concentrations that have no effect on gramicidin channel function (Sawyer et al, 1990). Single-channel experiments were done at 25 ± 1 °C using the bilayer punch method with pipette tip diameters ~30 μm (Andersen, 1983) and a Dagan 3900 patch clamp amplifier (Dagan Corp., Minneapolis, MN). The current signal was filtered at 5000 Hz (Frequency Devices, Haverhill, MA), digitized and digitally filtered to 500 Hz for analysis.

Single-channel current transitions were detected using a current-transition detection algorithm

(Andersen, 1983) implemented in Visual Basic. To facilitate the determination of appearance rates and lifetimes of the different channel types, we first constructed single-channel current transition amplitude histograms based on the magnitude of the difference in current levels before and after a current transition (Andersen, 1983), such that the transitions associated with each channel type appears as a single peak in the histograms. The lifetime histograms then were constructed as previously described (Andersen, 1983; Sawyer et al., 1989). The lifetime histograms were transformed into survivor distributions, and the average channel lifetimes ($\tau = 1/k_{-1}$) were determined by fitting a single exponential distribution: $N(t) = N(0) \cdot \exp\{-t/\tau\}$, where $N(t)$ denotes the number of channels with a lifetime longer than time t, to each survivor distribution.

To quantify the effect of BDM on the channel appearance rate, $f (= k_1 \cdot [M]^2)$, we determined the channel appearance rates using the bilayer punch method based on the average appearance rates from two (5 – 10 min) recordings obtained before and 10 – 20 min after BDM addition. Only bilayers that did not break during BDM addition were used for this analysis.

Relative changes in the time-averaged channel "concentrations" were determined as the ratio the product of the channel appearance rate and lifetime – measured before and after the addition of BDM (cf. Scheme I; see Andersen et al, 2006, for derivation):

$$\frac{[D]_{BDM}}{[D]_{cntrl}} = \frac{f_{BDM} \cdot \tau_{BDM}}{f_{cntrl} \cdot \tau_{cntrl}} = \frac{k_{1,BDM} \cdot [M]^2_{BDM} / k_{-1,BDM}}{k_{1,cntrl} \cdot [M]^2_{cntrl} / k_{-1,cntrl}} = \frac{K_{D,BDM}}{K_{D,cntrl}}, \tag{2}$$

where the subscripts "BDM" and "cntrl" denote the rate constants (cf. Scheme I) and appearance rates and lifetimes in the presence and absence of BDM, and the third equality holds in the limit $[M] \gg [D]$, such that $[M]_{BDM} \approx [M]_{cntrl}$. Changes in the free energy of gramicidin channel formation, $\Delta\Delta G^0_{tot}$, which should be equal to the BDM-induced change in ΔG^0_{def}, then was evaluated as:

$$\Delta\Delta G_{\text{tot}}^0 \ (\approx \Delta\Delta G_{\text{def}}^0) = -RT \cdot \ln\left\{\frac{K_{\text{D,BDM}}}{K_{\text{D,cntrl}}}\right\} = -RT \cdot \ln\left\{\frac{f_{\text{BDM}} \cdot \tau_{\text{BDM}}}{f_{\text{cntrl}} \cdot \tau_{\text{cntrl}}}\right\}, \tag{3}$$

where R is the gas constant and T temperature in Kelvin. Again, only bilayers that did not break during BDM addition were used for this analysis.

The final results for a given experimental condition are based on the mean ± standard deviation (SD) based on at least three independent measurements.

RESULTS

BDM modulation of CFTR channels in guinea pig ventricular myocytes

BDM elicited two types of responses in whole-cell CFTR Cl⁻ currents (I_{CFTR}), depending on how the drug was applied (Fig. 2).

Fig. 2A shows the current recorded from a ventricular myocyte at 0 mV, where the first of two successive applications of forskolin (an adenylyl cyclase agonist) activated a large I_{CFTR} (outward current at 0 mV), which deactivated following removal of forskolin. Addition of 20 mM BDM to resting CFTR channels had no effect on the whole-cell current, but the response to forskolin was diminished by 76 ± 6 % ($I_{CFTR}^{BDM} / I_{CFTR}^{Cntrl}$, where the superscripts denote the forskolin-induced currents in the presence and absence of BDM; $n = 4$) when added in the presence of BDM. Moreover, a distinct, biphasic response was observed when BDM was added in the presence of forskolin after I_{CFTR} was activated (second BDM application in Fig. 2B). The early phase was a rapid current increase (2.0 ± 0.3 fold increase in (peak I_{CFTR}^{BDM})/(steady state I_{CFTR}^{Cntrl}); $n = 6$), apparently rate limited by solution exchange. The late phase was a slower ($\tau = 20 \pm 6$ s, n = 5) current inhibition (by 81 ± 5 %; (steady state I_{CFTR}^{BDM})/(peak I_{CFTR}^{BDM})). Note that when added simultaneously with forskolin (first BDM application, Fig. 2B), the current enhancement by BDM was minimal, because the dominating effect was the inhibition that began while CFTR had not yet been activated (as in Fig. 2A). Thus, to observe the biphasic response, it was necessary to apply BDM with relatively fast solution exchange, after CFTR had been activated. The inhibitory effect of BDM (applied before or in the presence of forskolin) was observed in 10 out of 11 myocytes.

The slow inhibitory phase is consistent with BDM's reported enhancement of dephosphorylation in the heart (Wiggins et al, 1980), which may reflect activation of endogenous phosphatases rather than direct BDM-catalyzed dephosphorylation (Zimmermann et al, 1996). To test whether

the BDM-induced reduction of I_{CFTR} might be due to activation of endogenous protein phosphatases, we examined whether microcystin-LR, a potent inhibitor of protein phosphatase 1 (PP1) and protein phosphatase 2A (PP2A) (Yoshizawa et al, 1990) modified the inhibitory phase (Fig. 3).

Following two brief exposures to forskolin, addition of BDM during a third CFTR activation caused the biphasic response described above, with a rapid increase followed by a slower decrease in current. (Due to incomplete inhibition at 20 mM, withdrawal of BDM induced a rapid reduction in current, due to the loss of current stimulation, followed by a slow recovery from inhibition, illustrating the complexity of the CFTR response to BDM.) The slow inhibitory phase was strongly attenuated during a second application of BDM ~10 min after intracellular perfusion of 10 μM microcystin (the larger forskolin-induced I_{CFTR}, which deactivated only partially, is due to microcystin effects prior to the BDM application). In all 7 experiments in which BDM was applied following intracellular perfusion with microcystin, we observed only the rapid I_{CFTR} enhancement, with minimal inhibitory effect. We conclude that distinct mechanisms underlie the two effects of BDM and that only its inhibitory effect reflects promotion of channel deactivation through BDM's stimulation of endogenous phosphatase activity.

Consistent with inhibition involving cytoplasmic constituents, application of BDM to giant inside-out patches caused only an increase in the open probability (P_O) of single CFTR channels (Fig. 4). The upper trace in Fig. 4A shows a recording from a patch in which joint application of PKA and ATP activated two CFTR channels with the characteristic high P_O of cardiac CFTR channels (Gadsby and Nairn, 1999); addition of 20 mM BDM therefore caused only a small further increase in P_O (Fig. 4B). The maneuver was repeated in the middle trace, with identical results. Withdrawal of PKA in the presence of ATP (lower record Fig. 4A) caused the usual

reduction in P_O, which is attributed to partial dephosphorylation of CFTR channels (Hwang et al., 1994); exposing such partially dephosphorylated channels to BDM caused a ~3-fold increase in P_O (Fig. 4B).

BDM activation of epithelial CFTR channels.

BDM affects many other ion channels and transporters in the membrane of ventricular myocytes (see Table 1, below). We therefore also examined the effects of BDM on human epithelial CFTR channels expressed in *Xenopus* oocytes using two-microelectrode voltage clamp (Figs. 5 and 6). We first examined the concentration dependence of BDM's action under conditions in which the channels were either weakly or strongly phosphorylated (Fig. 5).

CFTR channels expressed in *Xenopus* oocytes show a low level of basal activity, corresponding to a measurable level of phosphorylation, even without PKA stimulation (Csanády et al, 2005). As shown in Fig. 5A, stepwise increasing [BDM] at a holding potential of -30 mV progressively increased the inward current (inward because -30 mV is negative to the Cl^- equilibrium potential in oocytes), an effect that reversed with BDM withdrawal. After current deactivation, forskolin was applied along with cantharidin (CANT), a membrane permeant inhibitor of PP1 and PP2A (Honkanen, 1993), which led to a larger I_{CFTR} activation than was observed with forskolin alone. Increasing [BDM] under this strongly phosphorylating condition also caused I_{CFTR} activation; the fractional increase in current (1.5 ± 0.1 fold; *n*=5) was less than that obtained with basal CFTR phosphorylation (18 ± 4 fold; *n*=5), and was evident at lower [BDM]. The membrane conductance was estimated from steady-state current-voltage curves (Fig. 5B), and is plotted against [BDM] in Fig. 5C. The extent of the BDM-induced increase in conductance was larger for basally phosphorylated channels (consistent with the results in Fig. 4) and the [BDM] for half-maximal effect ($K_{0.5}$) was ~10-fold higher ($K_{0.5} = 18 \pm 2$ mM, n = 4) than that observed in

the presence of cantharidin and forskolin ($K_{0.5}= 2 \pm 0.3$ mM, n = 5). BDM did not increase the conductance of uninjected oocytes (Allen et al., 1998; see also Supplementary Figure 1).

The CFTR activating effect of BDM resembles that of genistein (Weinreich et al, 1997) and capsaicin (Ai et al, 2004), which do not enhance the activity of fully dephosphorylated CFTR channels. As already suggested in Fig. 2A, phosphorylation seems to be required also for the BDM-induced enhancement of CFTR channel; this was further tested in oocytes by applying BDM before and after inhibition of PKA with its peptide inhibitor (PKI, Fig. 6).

In the maintained presence of forskolin, a brief exposure to BDM elicited a rapid and reversible increase in inward current (Fig. 6A), the CFTR conductance remained higher than the initial level despite evidence of the inhibitory effect described in the experiments with ventricular myocytes. Injection of PKI (arrow) slowly reduced I_{CFTR} (because the slow dephosphorylation of the channels could not be counteracted by the inhibited PKA), and a second application of BDM (≥ 15 min after PKI injection) no longer increased the conductance. Fig. 6B summarizes results from oocytes where 10 or 30 mM BDM were applied before and after PKI injection. Control experiments in which BDM was applied following injection with water instead of PKI always showed the usual I_{CFTR} activation (results not shown).

Enhancement of CFTR activity is not the only action shared by BDM capsaicin and genistein (see Table 1). Like capsaicin and genistein, BDM alters the function of many different membrane proteins – in a manner that does not appear to involve changes in protein phosphorylation. These observations raise the question, whether the amphipathic BDM might alter membrane protein function by some common, bilayer-dependent mechanism, as it has been proposed for genistein and capsaicin (Hwang et al, 2003; Lundbæk et al, 2005). To explore this question, we used gramicidin (gA) channels as molecular force transducers. (Andersen et al.,

1999), and studied the effect of BDM on the appearance and dissociation rates of gramicidin channels of different lengths and helix sense.

BDM modulation of gramicidin channel function

BDM increases gramicidin channels' activity (the time-averaged number of conducting channels) in DOPC/n-decane bilayers (Fig. 7), which primarily results from an increase in the channel appearance rate (see below). In these experiments, we incorporated AgA(15) and gA$^-$(13), two gramicidin analogues with different hydrophobic lengths (l), but different helix sense, in the same membrane. Because the two analogues form channels that have opposite helix sense they do not form heterodimers, and because the homodimers have different current transition amplitudes (as shown in Figs. 7 and 8) it is possible to analyze traces from membranes containing these two types of channels simultaneously (e.g. Lundbæk et al, 2005). Thus, the influence of the hydrophobic mismatch ($d_0 - l$) on the effects of BDM can be monitored in the same membrane under identical conditions. As seen in the current transition amplitude histograms (Fig. 8) and lifetime distributions (Fig. 9), in both the absence and presence of BDM we observed two different channel types, corresponding to the homodimeric AgA(15) and gA$^-$(13) channels. BDM had little effect on single-channel current transition amplitudes (Fig. 8), but caused a significant increase in the channel lifetimes (Fig. 9). In addition to its effect on gramicidin channel activity, BDM also caused subtle bilayer instability, as evident in the baselines in the presence of 10 and 20 mM BDM, and an increase in the background current through the bilayer (in the absence of gramicidin). No channel activity was observed in the absence of gramicidin, however, and we did not examine this issue further.

To examine whether the increase in gramicidin channel lifetime could result from specific BDM/bilayer-gramicidin channel interactions, we determined the effects on channels formed by the AgA(15) enantiomer AgA$^-$(15). Enantiomeric pairs of gramicidins form channels of

different helix sense (Koeppe et al., 1992), and specific channel-drug-bilayer interactions would

be expected to cause different effects on the two channels types. BDM caused similar

concentration-dependent increases in AgA$^-$(15) channel lifetimes, as it did in the case of the

AgA(15) and gA$^-$(13) channels (Fig. 10). The effect of BDM does not appear to depend on

specific BDM-gramicidin-lipid interactions. Nor is the effect of BDM on channel lifetime

enhanced in the case of the gA$^-$(13) channels, which have the bigger hydrophobic mismatch.

When a bilayer-spanning gramicidin dimer forms, the two bilayer leaflets will locally compress

and bend (Huang, 1986; Sawyer et al., 1989; Lundbæk and Andersen, 1994); in reaction, the

bilayer pulls on the dimer with a disjoining force, F_{dis} ($= -\partial \Delta G_{def}^0 / \partial (d_0 - l)$), and the channel

lifetime will vary as a function of F_{dis} (i.e. of ΔG_{def}^0). As gramicidin channels dissociate, they

reach the transition state for dissociation when the two subunits have moved a distance

δ (≈ 1.6 Å) apart (Durkin et al., 1993). The ΔG_{def}^0-dependent contribution to the transition

energy barrier may be calculated by subtracting ΔG_{def}^0 for the dimer (with hydrophobic mismatch

d_0-l) from ΔG_{def}^0 for the transition state (with hydrophobic mismatch d_0-l+δ), cf. Scheme I and

Eq. 1:

$$\begin{aligned}
\Delta\Delta G_{D\to M}^{\ddagger} &= H_B \cdot (d_0 - l + \delta)^2 + H_X \cdot (d_0 - l + \delta) \cdot c_0 + H_C \cdot c_0^2 \\
&\quad - H_B \cdot (d_0 - l)^2 - H_X \cdot (d_0 - l) \cdot c_0 - H_C \cdot c_0^2 \\
&= H_B \cdot (2 \cdot (d_0 - l) + \delta) \cdot \delta + H_X \cdot \delta \cdot c_0
\end{aligned} \tag{4}$$

Thus, changes in the energetics of channel formation, ΔG_{def}^0, and the kinetics of channel

dissociation, $\Delta\Delta G_{D\to M}^{\ddagger}$, induced by a drug could result from changes in bilayer thickness, d_0,

intrinsic lipid curvature, c_0, and the elastic moduli, as reflected in H_B and H_X – where H_B and H_X

(negative) vary more or less in parallel, as can be deduced from Eqs. 17 and 28 in (Nielsen and

Andersen, 2000).

To examine whether the BDM-induced increases in gramicidin channel lifetimes are associated

with a decrease in d_0, we estimated the changes in bilayer hydrophobic thickness from capacitance measurements on DOPC/n-decane bilayers (Lundbæk and Andersen, 1994). In the absence or presence of 20 mM BDM, the bilayer specific capacitance was 3.76 ± 0.08 nF/cm^2 (n=4) and 3.69 ± 0.08 nF/cm^2 (n=7), respectively. The invariant capacitance is consistent with the lack of effect of BDM on the linear capacitance of whole-cell ventricular myocytes (Ferreira et al, 1997). We conclude that BDM does not change hydrophobic thickness.

The increase in gramicidin channel lifetime therefore is due to decreased bilayer stiffness (decreased magnitude of H_B and H_X) or a more positive intrinsic curvature, c_0. To distinguish between these possibilities, we compared the relative lifetime changes for channels formed by AgA(15), AgA$^-$(15) and gA$^-$(13). The longer AgA(15) and AgA$^-$(15) channels have the longer lifetime, reflecting their smaller hydrophobic mismatch, as compared to the shorter gA$^-$(13), as well as the different amino acid sequences at the subunit interface in the different channels, which also contribute toward determining the single-channel lifetime (Mattice et al., 1995). Remarkably, and in contrast to results obtained in previous studies with other modifiers of bilayer elastic properties (Lundbæk and Andersen, 1994; Lundbæk et al., 2005), the relative changes in gA$^-$(13) channel lifetimes were comparable to (if anything less than) the changes observed with AgA(15) and AgA$^-$(15) channels (Fig. 10). These results suggest that the changes in gramicidin channel activity (bilayer stiffness) do not result from changes in bilayer elasticity, but rather from changes in intrinsic lipid curvature, c_0.

In contrast to the comparable lifetime changes, the BDM-induced increases in the appearance rates for the shorter gA$^-$(13) channels were larger than the increase in the appearance rates for the longer AgA(15) channels (Fig. 11).

The larger effect on the gA⁻(13) channels, compared to the AgA(15) channels, again can be understood by examining the contributions to the transition energy barrier for channel formation (subtracting ΔG_{def}^0 for the monomer (with a hydrophobic mismatch of 0) from ΔG_{def}^0 for the transition state), cf. Scheme I and Eq. 1:

$$
\begin{aligned}
\Delta\Delta G_{\text{M}\to\text{D}}^{\ddagger} &= H_{\text{B}}\cdot(d_0-l+\delta)^2 + H_{\text{X}}\cdot(d_0-l+\delta)\cdot c_0 + H_{\text{C}}\cdot c_0^2 - H_{\text{C}}\cdot c_0^2 \\
&= H_{\text{B}}\cdot(d_0-l+\delta)^2 + H_{\text{X}}\cdot(d_0-l+\delta)\cdot c_0
\end{aligned}
\tag{5}
$$

Comparing Eqs. 4 and 5, the curvature-dependent contribution to the kinetics of channel dissociation (the $H_{\text{X}}\cdot\delta\cdot c_0$ term in $\Delta\Delta G_{\text{D}\to\text{M}}^{\ddagger}$, Eq. 4) does not depend on the channel-bilayer hydrophobic mismatch *per se*. In contrast, the curvature-dependent contribution to the kinetics of channel formation (the $H_{\text{X}}\cdot(2\cdot(d_0-l)+\delta)\cdot c_0$ term in $\Delta\Delta G_{\text{M}\to\text{D}}^{\ddagger}$) will vary with channel-bilayer hydrophobic mismatch, $d_0 - l$, which accounts for the larger relative changes in appearance rates for the gA⁻(13) channels as compared to the AgA(15). Moreover, the relative changes in the appearance rates will be larger than the changes in the lifetimes whenever $d_0 - l - \delta > \delta$, cf. Lundbæk et al. (2005).

As would be expected from the results in Figs. 10 and 11, the time-averaged increase in channel concentrations was larger in the case of gA⁻(13) channels, as compared to AgA(15) channels (Fig. 12).

Given the relative changes in the time-averaged channel concentrations, we can estimate the changes in the free energy of channel formation, $\Delta\Delta G_{\text{tot}}^0$ (cf. Eq. 3). The results are shown in Fig. 12 (the right-hand ordinate). We conclude that BDM alters the free energy of gramicidin channel formation, and that the changes in $\Delta\Delta G_{\text{tot}}^0 \approx \Delta\Delta G_{\text{def}}^0$ most likely result from changes in intrinsic lipid curvature – as might have been expected for the adsorption of small, compact amphipathic molecules that are likely to reside at the bilayer/solution interface. Though we cannot exclude that BDM alters other bilayer properties, such as "fluidity", our results provide

no support for such changes – and changes in "fluidity" would not cause the $\Delta\Delta G^0$ changes we observe (i.e. changes in fluidity would affect the appearance rate and the dissociation rate $(1/\tau)$ in the same direction).

DISCUSSION

In this study, we extend the number of integral membrane proteins whose functions are modified by BDM at comparable [BDM]s (Table 1). Though some BDM effects may be related to the target protein's phosphorylation status (e.g. Chapman, 1993; Xiao and McArdle, 1995), others appear to be phosphorylation-independent (e.g. Lopatin and Nichols, 1993; Watanabe et al., 2001) – and, as shown here, some proteins can be modified by a combination of phosphorylation-dependent and –independent mechanisms.

The phosphorylation-independent effects are likely to result because BDM is a general modifier of bilayer material properties (thickness, intrinsic curvature, and elastic properties), as evident by its effects on gramicidin channels at the same [BDM] used to manipulate integral membrane protein function. Though the conformational transitions underlying the gating of CFTR and gramicidin channels are different, the BDM-induced changes in gramicidin channel function provides an explanation for BDM's seemingly nonspecific modification of membrane protein function.

Effects on CFTR channel function

BDM alters CFTR function by two apparently independent and opposite mechanisms: a fast, phosphorylation-independent activation; and a slower, seemingly dephosphorylation-dependent inhibition (through deactivation). Observations on L-type Ca channels illustrate the difficulty of deciding whether BDM's actions are phosphorylation-mediated: Chapman (1993) showed that channel inhibition by BDM was antagonized by isoprenaline stimulation, as if it involved dephosphorylation of PKA-dependent sites; Allen et al. (1998) reported similar BDM-induced inhibition of recombinant channels lacking all PKA consensus sites. Thus, mechanistically different processes may alter channel function in the same direction – impeding a clear separation of their individual contributions. In our case, it was the oppositely directed

dephosphorylation-dependent and dephosphorylation-independent effects of BDM on CFTR channels that allowed us to distinguish between these mechanisms. Complex phosphorylation-independent effects of BDM on ryanodine receptors (RyRs), where BDM at low $[Ca^{2+}]$ activates both cardiac and skeletal muscle RyRs but at high $[Ca^{2+}]$) inhibits skeletal muscle RyR activity have been reported (Tripathy et al ,1999).

Dephosphorylation-mediated inhibition of CFTR. Cardiac whole-cell CFTR currents were inhibited by BDM, whether or not BDM was applied before or after adenylate cyclase activation by forskolin. 20 mM BDM caused an 80% inhibition, meaning that the K_I for this effect is ~ 5 mM, similar to other membrane proteins (Table I). Microcystin, a potent inhibitor of PP1 and PP2A, largely abolished BDM's inhibition of I_{CFTR}, suggesting that BDM activates endogenous phosphatases, cf. Zimmerman et al (1996), who showed that cantharidin antagonized BDM-induced phosphatase activity in mammalian heart.

BDM did not inhibit CFTR channels in excised patches, a surprising result in light of reports of direct PP2A-CFTR interactions in Calu-3 cells (Thellin et al, 2005). Assuming similar interactions in cardiomyocytes, the lack of BDM effect may indicate that the BDM-induced I_{CFTR} inhibition caused by PP1/PP2A activation is lost in inside-out excised patches. But these recordings were done at room temperature, whereas the whole-cell recordings were done at 36-37 °C, and it is possible that phosphatase activation by BDM is accentuated at higher temperatures, cf. Stapleton et al (1998). The lack of clear inhibitory effect in oocytes, similarly may be related to the lower temperatures used in these experiments.

Phosphorylation-independent stimulation of CFTR current. The transient ~2-fold increase in the whole-cell cardiomyocyte I_{CFTR} (Figs. 2 and 3) agrees with the BDM-induced enhancement of channel activity in inside-out patches (Fig. 4), where P_O increases ~1.2-fold for highly

phosphorylated, and ~3-fold for moderately phosphorylated channels. Similarly to the CFTR stimulation by genistein and capsaicin (Ai et al, 2004), stimulation of CFTR by BDM requires at least partially phosphorylated channels. That said, the BDM-dependent raise in P_O does not reflect an increase in phosphorylation, as it occurs in the absence of PKA.

The changes in channel function induced by the structurally dissimilar (Supplemantary Figure 2) BDM, capsaicin and genistein go far beyond CFTR (Table I). These compounds induce analogous responses on many unrelated membrane proteins, including voltage-dependent ion channels, Na^+/Ca^{2+}-exchanger, mitochondrial Complex I and gramicidin channels. These pleiomorphic effects might arise because these different compounds bind directly to their different targets, but the parsimonious interpretation is that BDM, capsaicin and genistein exert their effects by a common mechanism involving the lipid bilayer.

BDM alters bilayer material properties

As previously shown for genistein (Hwang et al., 2003) and capsaicin (Lundbæk et al., 2005), BDM shifts the equilibrium distribution between non-conducting monomers and conducting dimers in favor of the dimers, mainly by increasing channel appearance rate (k_1) (Fig. 11), with a smaller increase in lifetime (decrease in k_{-1}) (Fig. 10). Because BDM's alteration of the energetics of gramicidin channel formation depends on the channel-bilayer hydrophobic mismatch (Fig. 12) we conclude that it reflects BDM's alteration of the bilayer deformation energy.

In contrast to results with lysophospholipids (Lundbæk and Andersen, 1994), genistein (Hwang et al., 2003) and capsaicin (Lundbæk et al., 2005), however, the relative changes in lifetime induced by BDM do not depend on the hydrophobic mismatch (Fig. 10), contrary to what would be expected if BDM altered the elastic moduli (because H_B-dependent term in Eq. 4 depends on

the hydrophobic mismatch). This result suggests that the BDM-induced changes in the height of the activation energy barrier for channel dissociation primarily result from changes in the intrinsic lipid curvature (c_0). (We do not, however, have independent measurements of how BDM alters c_0.)

Is the BDM stimulation of CFTR a pure bilayer effect? Previous data (Hwang et al., 2003; Ai et al., 2004; Lundbæk et al., 2005) show that some amphipathic molecules alter CFTR function at the concentrations where they affect bilayer material properties, as monitored using gramicidin channels. Moreover, BDM appears to be a promiscuous modifier of membrane protein function at the concentrations used in the present experiments (Table I). Taken together, these results suggest that BDM's effect on CFTR function indeed is a bilayer-mediated effect, but we cannot exclude that the BDM-induced changes in CFTR function also could result from some specific interactions with CFTR, similar to those proposed for capsaicin and genistein (Ai et al, 2004). Indeed, one would expect that amphipathic compounds could alter membrane protein function by a combination of specific interactions with the target protein and bilayer-mediated interactions. The relative importance of these effects will depend on amphiphile structure and the protein conformational changes. Studies with other modifiers of bilayer material properties will be needed to determine whether all inducers of positive curvature c_0 enhance I_{CFTR}, and to elucidate the relative importance of changes in curvature and bilayer elastic moduli. Remarkably, polyunsaturated fatty acids (inducers of negative curvature) inhibit epithelial Cl^- currents (Hwang et al, 1990).

It is in this context important that, though the absolute changes in intrinsic curvature (or elastic moduli) induced by BDM would be expected to vary with the bilayer composition, the *direction* of the changes should be invariant as the overall bilayer properties should be a weighted average of the properties of the individual lipid components (cf. Rand and Parsegian, 1997). (The

relevant radii of curvature are on the order of $1 - 10$ nm, such that the overall bilayer can be approximated as a flat sheet (meaning that the BMD-induced curvature changes do not depend on the experimental system, whole-cell vs. patch recording).) Finally, similar changes in c_0 have been proposed to alter the equilibrium distribution and activity of other membrane proteins, including protein kinase C (Slater et al, 1994). Though it remains to be seen whether BDM activation of endogenous phosphatases in ventricular myocytes is mediated by its apparent modification of intrinsic curvature, c_0 may be an even more general regulator of protein phosphorylation. Regardless of these uncertainties, however, a bilayer-mediated mechanism not only can account for CFTR's potentiation by BDM, genistein and capsaicin, it also can account for these compounds ability to alter the function of numerous, structurally unrelated proteins.

Modulated receptor and bilayer-mediated effects.

Amphiphiles that decrease lipid bilayers stiffness promote inactivation of voltage-dependent cation channels (Lundbæk et al, 2004; 2005) – with little effect on channel activation – leading to the suggestion that inactivated channel states may have a higher channel/bilayer hydrophobic mismatch than other channel states (Lundbæk et al, 2004). Likewise, BDM promotes voltage-dependent inactivation of cardiac potassium (Xiao and McArdle, 1995) and calcium channels (Ferreira et al, 1997). BDM, like genistein and capsaicin, enhance I_{CFTR} and induce a large potentiation of partially-phosphorylated channels with relatively minor effects on highly-phosphorylated channels (Ai et al, 2004). These compounds thus modify the equilibrium between preexisting low and high P_O states – which normally involves phosphorylation-dephosphorylation reactions. Because our experiments were done in presence of saturating [ATP], and ATP-dependent gating seems unaffected by genistein ($K_{0.5ATP}$ ~80 µM, Weinreich et al, 1997), these changes in P_O are unlikely to reflect changes in ATP binding at the nucleotide binding domains. Thus, by analogy with what was suggested for voltage-dependent sodium channels, CFTR states that display a higher P_O (under given experimental conditions) may have a

larger hydrophobic mismatch at the protein-bilayer interface. If the conformational change that activates the channels involves an increase in hydrophobic mismatch, with states having the maximal P_O having maximal mismatch, our observations can be explained by the modification of bilayer material properties in the absence of direct ligand-protein interaction.

For a given CFTR gating state, the distribution between closed and open channels can be approximated as:

$$P_O = \frac{1}{1 + \exp\{+\Delta G_{tot}^{C \to O} / RT\}}, \tag{6}$$

where $\Delta G_{tot}^{C \to O}$, by analogy with the situation for gramicidin channels, can be written as the sum of contributions arising from the protein per se, $\Delta G_{prot}^{C \to O}$, and from the difference in the bilayer deformation in the closed and open channels, $\Delta\Delta G_{def}^{C \to O} = \Delta G_{def}^{O} - \Delta G_{def}^{C}$. Channel states with higher P_O will have a more negative $\Delta\Delta G_{tot}^{C \to O}$ than states with lower P_O, but it is the sum of $\Delta G_{prot}^{C \to O}$ (negative) and $\Delta\Delta G_{def}^{C \to O}$ (positive, as it opposes channel activation) that determines P_O, and the relative effect of a given change in $\Delta\Delta G_{def}^{C \to O}$ will be greater at lower P_Os, as is observed. Within this scenario, the shift in the [BDM] needed for half maximal effect arises because displacing the equilibrium from a low P_O state (with a small hydrophobic mismatch) to a high P_O state (with a large hydrophobic mismatch), requires a larger reduction in $\Delta\Delta G_{def}^{C \to O}$, which requires a higher [BDM]. That is, modification of lipid bilayer properties, which requires no direct protein-ligand interactions, can explain the shifts in apparent affinities often attributed to direct protein-ligand interactions in the modulated receptor hypothesis (Hille, 2001).

Assuming that inactivated states have the highest, active states some intermediate, and resting states the lowest, hydrophobic mismatch, the same argument can explain the dual, Ca^{2+}-dependent modulation of skeletal muscle RyRs by BDM (Tripathy et al, 1999).

Conclusion

We show that BDM alters the function of yet another membrane protein at low mM concentrations, and provide a mechanism to account for its complex, yet seemingly nonspecific effects. By altering the lipid bilayer and activating endogenous phosphatases, BDM would be expected to alter the function of many membrane (as well as cytoplasmic) proteins at the concentration range at which it inhibits muscle myosin ATPase (concentration for half-maximal inhibition ~1 mM; Herrmann et al, 1992), which tends to invalidate its use as specific research tool. That said, BDM's inhibitory effects on myosin ATPase and membrane proteins such as the Na^+/Ca^{2+}-exchanger and calcium channels might well underlie BDM's beneficial effects in organ preservation for transplantation (Warnecke et al, 2002).

References

Ai T., S.G. Bompadre, X. Wang, S. Hu, M. Li, and T.C. Hwang. 2004. Capsaicin potentiates wild-type and mutant cystic fibrosis transmembrane conductance regulator chloride-channel currents. *Mol. Pharmacol.* **65**:1415-1426.

Allen T.J., G. Mikala, X.Wu, and A.C. Dolphin. 1998. Effects of 2,3-butanedione monoxime (BDM) on calcium channels expressed in Xenopus oocytes. *J. Physiol.* 508:1-14.

Andersen, O.S. 1983. Ion movement through gramicidin A channels. Single-channel measurements at very high potentials. *Biophys. J.* 41:119-133.

Andersen, O.S., C. Nielsen, A.M. Maer, J.A. Lundbæk, M. Goulian, and R.E. Koeppe, II. 1999. Ion channels as tools to monitor lipid bilayer-membrane protein interactions: gramicidin channels as molecular force transducers. *Meth. Enzymol.* 294:208-224.

Andersen, O.S., M.J. Bruno, H. Sun and R.E. Koeppe II. 2007. Single-molecule methods for monitoring changes in bilayer elastic properties. *Methods in Molecular Biology, in press.*

Baker L.C., R. Wolk, B.R. Choi, S. Watkins, P. Plan, A. Shah, and G. Salama. 2004. Effects of, mechanical uncouplers, diacetyl monoxime, and cytochalasin-D on the electrophysiology of perfused mouse hearts. *Am. J. Physiol. Heart Circ. Physiol.* **287**:H1771-1779.

Chan, K.W., L. Csanády, D. Seto-Young., A.C. Nairn, and D.C. Gadsby. 2000. Severed molecules functionally define the boundaries of the cystic fibrosis transmembrane conductance regulator's NH(2)-terminal nucleotide binding domain. *J. Gen. Physiol.* **116**:163-180.

Chapman, R.A. 1993. The effect of oximes on the dihydropyridine-sensitive Ca current of isolated guinea-pig ventricular myocytes. *Pflügers Arch.* **422**:325-31.

Csanády, L. 2000. Rapid kinetic analysis of multichannel records by a simultaneous fit to all dwell-time histograms. *Biophys. J.* **78**:785-799.

Csanády L., D. Seto-Young, K.W. Chan, C. Cenciarelli, B.B. Angel, J. Qin, D.T. McLachlin, A.N. Krutchinsky, B.T. Chait, A.C. Nairn, and D.C. Gadsby. 2005. Preferential phosphorylation of R-domain Serine 768 dampens activation of CFTR channels by PKA. J. Gen. Physiol. 125:171-186.

Durkin, J.T., L.L. Providence, R.E. Koeppe, II, and O.S. Andersen. 1993. Energetics of heterodimer formation among gramicidin analogues with an NH_2-terminal addition or deletion. Consequences of a missing residue at the join in channel. *J. Mol. Biol.* 231:1102-1121.

Evans, E., W. Rawicz, and A.F. Hofmann. 1995 . Lipid bilayer expansion and mechanical disruption in solutions of water-soluble bile acid. *In*: Bile Acids in Gastroenterology Basic and Clinical Advances. A.F. Hofmann, G. Paumgartner, and A. Stiehl, editors. Ed.

Kluwer Academic Publishers, Dordrecht. 59-68.

Evans, E.A. and R.M. Hochmuth. 1978. Mechanochemical properties of membranes. *Curr. Top. Membr. Transp.* 10:1-64.

Ferreira, G., P. Artigas, G. Pizarro, and G. Brum. 1997. Butanedione monoxime promotes voltage-dependent inactivation of L-type calcium channels in heart. Effects on gating currents. *J. Mol. Cell. Cardiol.* 29:777-787.

Gadsby, D.C, and A.C. Nairn. 1999. Control of CFTR channel gating by phosphorylation and nucleotide hydrolysis. *Physiol. Rev.* 79:S77-S107.

Greathouse, D.V., R.E. Koeppe, II, L.L. Providence, S. Shobana, and O.S. Andersen. 1999. Design and characterization of gramicidin channels. *Meth. Enzymol.* 294:525-550.

Gruner, S.M. 1985. Intrinsic curvature hypothesis for biomembrane lipid composition: a role for nonbilayer lipids. *Proc. Natl. Acad. Sci. USA* 82:3665-3669.

Gruner, S.M. 1991. Lipid membrane curvature elasticity and protein function. *In*: Biologically Inspired Physics. L. Peliti, editor. Ed. Plenum Press, New York. 127-135.

Herrmann, C; Wray, J; Travers, F and Barman, T. 1992. Effect of 2,3-Butanedione Monoxime on Myosin and Myofibrillar ATPases. An Example of an Uncompetitive Inhibitor? *Biochemistry* 31: 12227-12232

Higuchi, H and S. Takemori. 1989. Butanedione monoxime suppresses contraction and ATPase activity of rabbit skeletal muscle. *J. Biochem.* (Tokyo) 105:638-43.

Holmstedt, B. 1959. Pharmacology of organophosphorus cholinesterase inhibitors. *Pharmacol. Rev.* 11:567–688.

Honkanen, R.E. 1993. Cantharidin, another natural toxin that inhibits the activity of serine/threonine protein phosphatases types 1 and 2A. *FEBS Lett.* 330:283-286.

Huang, H.W. 1986. Deformation free energy of bilayer membrane and its effect on gramicidin channel lifetime. *Biophys. J.* 50:1061-1070.

Hwang TC, S.E. Guggino and W.B. Guggino. 1990. Direct modulation of secretory chloride channels by arachidonic and other cis unsaturated fatty acids. *Proc. Natl. Acad. Sci. U S A.* **87**:5706-5709.

Hwang, T.C., M. Horie, and D.C. Gadsby. 1993 Functionally distinct phospho-forms underlie incremental activation of protein kinase-regulated Cl- conductance in mammalian heart. *J. Gen. Physiol.* 101:629-650.

Hwang T.C., G. Nagel, A.C. Nairn, and D.C. Gadsby. 1994. Regulation of the gating of cystic fibrosis transmembrane conductance regulator C1 channels by phosphorylation and ATP hydrolysis. *Proc. Nat.l Acad. Sci. U S A.* 91:4698-4702.

Hwang, T.C., R.E. Koeppe II, and O.S. Andersen. 2003. Genistein can modulate channel function by a phosphorylation-independent mechanism: importance of hydrophobic mismatch and bilayer mechanics. *Biochemistry* 42:13646-13658.

Koeppe, R.E., II, L.L. Providence, D.V. Greathouse, F. Heitz, Y. Trudelle, N. Purdie, and O.S. Andersen. 1992. On the helix sense of gramicidin A single channels. *Proteins* 12:49-62.

Lee, A.G. 2003. Lipid-protein interactions in biological membranes: a structural perspective. *Biochim. Biophys. Acta* 1612:1-40.

Lopatin, A.N. and C.G. Nichols. 1993. 2,3-Butanedione monoxime (BDM) inhibition of delayed rectifier DRK1 (Kv2.1) potassium channels expressed in Xenopus oocytes. *J. Pharmacol. Exp. Ther.* 265:1011-1016.

Lundbæk, J.A. and O.S. Andersen. 1994. Lysophospholipids modulate channel function by altering the mechanical properties of lipid bilayers. *J. Gen. Physiol.* 104:645-673.

Lundbæk JA, P. Birn, A.J. Hansen, R. Sogaard, C. Nielsen, J. Girshman, M.J. Bruno, S.E. Tape, J. Egebjerg, D.V. Greathouse, G.L. Mattice, R.E. Koeppe II and O.S. Andersen. 2004. Regulation of sodium channel function by bilayer elasticity: the importance of hydrophobic coupling. Effects of Micelle-forming amphiphiles and cholesterol. *J. Gen. Physiol.* 123:599-621.

Lundbæk, J.A., P. Birn, S.E. Tape, G.E. Toombes, R. Sogaard, R.E. Koeppe II, S.M. Gruner, A.J. Hansen, and O.S. Andersen. 2005. Capsaicin regulates voltage-dependent sodium channels by altering lipid bilayer elasticity. *Mol. Pharmacol.* 68:680-689.

Ly, H.V. and M.L. Longo. 2004. The influence of short-chain alcohols on interfacial tension, mechanical properties, area/molecule, and permeability of fluid lipid bilayers. *Biophys. J.* 87:1013-1033.

Mattice G.L., R.E. Koeppe II, L.L. Providence and O.S. Andersen. 1995. Stabilizing effect of D-alanine2 in gramicidin channels. *Biochemistry* 34:6827-6837.

Mouritsen, O.G. and M. Bloom. 1984. Mattress model of lipid-protein interactions in membranes. *Biophys. J.* 46:141-153.

Nielsen, C. and O.S. Andersen. 2000. Inclusion-induced bilayer deformations: effects of monolayer equilibrium curvature. *Biophys. J.* 79:2583-2604.

Rand, R.P. and V.A. Parsegian. 1997. Hydration, curvature, and bending elasticity of phospholipid monolayers. *Curr. Topics Mem. Transp.* 44:167-189.

Sackmann, E. 1984. Physical basis of trigger processes and membrane structures. *In*: Biological Membranes. D. Chapman, editor. Editor. Academic Press Inc., Ltd., London. 105-143.

Sawyer, D.B., R.E. Koeppe, II, and O.S. Andersen. 1989. Induction of conductance heterogeneity in gramicidin channels. *Biochemistry* 28:6571-6583.

Sawyer, D.B., R.E. Koeppe, II, and O.S. Andersen. 1990. Gramicidin single-channel properties show no solvent-history dependence. *Biophys. J.* 57:515-523.

Slater, S. J., Kelly, M. B., Taddeo, F. J., Rubin, E., and C.D. Stubbs. 1994 The modulation of protein kinase C activity by membrane lipid bilayer structure. *J. Biol. Chem.* **269:** 17160-17165.

Stapleton MT, Fuchsbauer CM, Allshire AP. 1998. BDM drives protein dephosphorylation and inhibits adenine nucleotide exchange in cardiomyocytes. *Am. J. Physiol.* 275:H1260-H1266

Sellin, L.C. and J.J. McArdle. 1994. Multiple effects of 2,3-butanedione monoxime. *Pharmacol. Toxicol.* 74:305-313.

Thellin, WR, M. Kesimer, R. Tarran, S.M. Kreda, B.R. Grubb, J.K. Sheehan, M.J. Stutts and S.L. Milgram. 2005. The cystic fibrosis transmembrane conductance regulator is regulated by a direct interaction with the protein phosphatase 2A. *J Biol Chem.* 280:41512-41520.

Titus, M.A. 2003. Caveat experimentor--is your myosin really inhibited? *Nat. Cell. Biol.* **5**: 95.

Tripathy A., L. Xu, D.A. Pasek and G. Meissner. 1999. Effects of 2,3-butanedione 2-monoxime on Ca2+ release channels (ryanodine receptors) of cardiac and skeletal muscle. *J. Membr. Biol.* **169**:189-198

Warnecke G., B. Schulze, C. Hagl, A. Haverich and U. Klima. 2002. Improved right heart function after myocardial preservation with 2,3-butanedione 2-monoxime in a porcine model of allogenic heart transplantation. *J. Thorac. Cardiovasc. Surg.* **123**:81-88.

Watanabe, Y., T. Iwamoto, I. Matsuoka, S. Ohkubo, T. Ono, T. Watano, M. Shigekawa, and J. Kimura. 2001. Inhibitory effect of 2,3-butanedione monoxime (BDM) on Na(+)/Ca(2+) exchange current in guinea-pig cardiac ventricular myocytes. *Br. J. Pharmacol.* 132:1317-1325

Weinreich, F., P.G.Wood, J.R. Riordan, and G. Nagel. 1997. Direct action of genistein on CFTR. *Pflügers Arch.* 434:484-491.

Wiggins J.R., J. Reiser, D.F. Fitzpatrick, and J.L.F. Bergey. 1980. Inotropic actions of diacetyl monoxime in cat ventricular muscle. *J. Pharmacol. Exp. Ther.* 212:217-224.

Xiao, Y.F. and McArdle, J.J. 1995. Activation of protein kinase A partially reverses the effects of 2,3-butanedione monoxime on the transient outward K+ current of rat ventricular myocytes. *Life Sci.* **57**:335-343

Yoshizawa, S., R. Matsushima, M.F. Watanabe, K. Harada, A. Ichihara, W.W. Carmichael, and H. Fujiki. 1990. Inhibition of protein phosphatases by microcystins and nodularin associated with hepatotoxicity. *J. Cancer Res. Clin. Oncol.* 116:609-614.

Zimmermann, N, P. Boknik, E. Gams, S. Gsell, L.R. Jones, R. Maas, J. Neumann, and H. Scholz. 1996. Mechanisms of the contractile effects of 2,3-butanedione-monoxime in the mammalian heart. *Naunyn Schmiedebergs Arch. Pharmacol*. 354:431-436.

Footnotes

FIGURE LEGENDS

Figure 1: Schematic representation of an ion channel protein in the lipid bilayer as it changes its conformation from closed (top) to open (bottom). Channel opening makes the channel hydrophobic length (l) shorter than the bilayer hydrophobic thickness (d_0), inducing compression and bending of the lipid bilayer around the channel. (The actual conformational changes may involve other types of perturbation of the lipid packing around the channel.) The energetic cost of membrane deformation (see text) depends on the hydrophobic mismatch (d_0-l). A similar deformation occurs when a gramicidin channel forms (cf. Lundbæk et al., 1994; 2004; 2005).

Figure 2: Dual effect of BDM on I_{CFTR} in cardiac myocytes. **A**, continuous whole-cell current recording at 36°C from a ventricular myocyte held at 0 mV and exposed to 2 μM forskolin (FSK) and/or 20 mM BDM (indicated by horizontal bars). Vertical current deflections correspond to application of 80 ms-long voltage steps to different voltages. **B**, whole-cell recording from a myocyte exposed to 2 μM forskolin with or without simultaneous application of 20 mM BDM. The grey line denotes a single exponential fit to the decay phase of I_{CFTR} following a second application of BDM (τ = 13.3 s; maximal I_{CFTR} = 250 pA, steady state I_{CFTR} = 39 pA).

Figure 3: Different mechanisms underlie current enhancement and current inhibition by BDM. Whole-cell recording from a myocyte held at 0 mV, which was exposed several times to 2 μM forskolin and/or 20 mM BDM (indicated by bars), before and after intracellular perfusion with 10 μM microcystin. The grey line denotes a single exponential fit to the current decay induced by BDM (τ = 44 s; maximal I_{CFTR} = 520 pA, steady state I_{CFTR} = 210 pA. Because the VCR tape ended before the end of the experiment, a scanned image from the chart recorded (dotted box) illustrates reversibility of BDM action after microcystin perfusion.

Figure 4: Activation of single cardiac CFTR channels. **A**, Two CFTR channels in a giant inside-out patch excised from a ventricular myocyte activated by cytoplasmic (bath) exposure to 2 mM MgATP and 200 nM PKA. *Top and middle trace*, 20 mM BDM applied in the presence of PKA and ATP increased the channels' P_O from 0.85 to 0.95. *Bottom trace*, after the reduction in P_o on PKA removal in 2 mM MgATP, 20 mM BDM increased P_O from 0.2 to 0.7. T= 22°C. **B**, average (± SEM) P_O from 3 different patches (with 2-4 channels each) in which BDM action was tested in 2 mM MgATP before and after withdrawal of PKA.

Figure 5: Concentration-dependence of BDM's effect on human epithelial CFTR expressed in *Xenopus* oocytes. **A**, response to progressive increments of [BDM] (holding potential −30 mV, CFTR activation increases the inward current) under two different conditions; after channel deactivation following the first application of forskolin (limited phosphorylation) and after stimulating phosphorylation with 40 μM forskolin (FSK) and 150 μM cantharidin (CANT). **B**, *I-V* curves obtained from the current near the end of 50-ms long rectangular voltage pulses; the letters indicate the corresponding times in A. The lines denote linear fits to the data between −70 and +40 mV. **C**, membrane conductance of the oocyte in A (from fits as in B) as a function of [BDM] when applied alone (solid squares) or with forskolin plus cantharidin (open circles). The curves are single-site binding isotherms fitted to the data, $g_0 + \Delta g_{max} \cdot [BDM]/(K_{0.5} + [BDM])$, with parameters g_0= 2.7 μS, Δg_{max}= 84 μS and $K_{0.5}$= 16 mM for BDM alone (solid) and g_0= 40 μS, Δg_{max}= 30 μS and $K_{0.5}$= 3 mM for BDM in the presence of forskolin and cantharidin (dashed).

Figure 6: BDM does not activate fully dephosphorylated channels. **A**, two days after injection with cRNA encoding for human epithelial CFTR, an oocyte held at −30 mV was exposed to 40 μM forskolin and then to 20 mM BDM before and after injection of 50 nl of 20 mM PKI to

inhibit PKA. **B**, summary of mean (±S.E.M.) effect of 10 or 30 mM BDM, expressed as conductance ratios, from experiments similar to that in A.

Figure 7: BDM increases gramicidin channel activity. Current traces recorded in the absence and presence of 10 or 20 mM BDM. Two different gramicidins, AgA(15) and gA$^-$(13), were present on both sides of the bilayer. The AgA(15)/AgA(15) and gA$^-$(13)/gA$^-$(13) homodimeric channels can be distinguished by virtue of their different current transition amplitudes, as indicated by the two horizontal lines (see also Fig. 8). No heterodimeric channels formed because the two gramicidin analogues have opposite chirality. The nominal concentration of gA$^-$(13), ~20 pM, was 10–fold larger than that of AgA(15), ~2 pM. 1.0 M NaCl, pH 7.0; 25 °C; 200 mV; 500 Hz.

Figure 8: BDM has little effect on the gramicidin current transition amplitudes. Current transition amplitude histograms obtained in the absence and presence of 10 or 20 mM BDM. The histograms are assembled from the current transition amplitudes, the absolute value of the difference in current level just before and just after a current transition (Andersen, 1983), and only the transition amplitudes are plotted. The histogram thus differs from a current level (or all-points) histogram. In each histogram there is two peaks, one around 2.1 pA and one around 3.3 pA corresponding to the gA$^-$(13) and the AgA(15) homodimeric channels, respectively. In the absence of BDM, there are 904 transitions in the histogram: 318 (or 35%) in the gA$^-$(13) channel peak at 2.06 ± 0.15 pA; and 491 (or 54%) in the AgA(15) channel peak at 3.21 ± 0.14 pA. In the presence of 10 mM BDM, there are 1149 transitions in the histogram: 563 (or 49%) in the gA$^-$(13) channel peak at 2.12 ± 0.15 pA; and 478 (or 42%) in the AgA(15) channel peak at 3.32 ± 0.17 pA. In the presence of 20 mM BDM, there are 1250 transitions in the histogram: 643 (or 51%) in the gA$^-$(13) channel peak at 2.17 ± 0.13 pA; and 477 (or 38%) in the AgA(15) channel peak at 3.42 ± 0.13 pA. In each histogram, we can account for ~90% of the current transitions.

The current transition amplitudes increase ~6% at 20 mM BDM, and there is gradual shift in the distribution between the shorter gA⁻(13) and the longer AgA(15) channels (see also Figs. 11 and 12). 1.0 M NaCl, pH 7.0; 25 °C; 200 mV; 500 Hz.

Figure 9: BDM increases gramicidin channel lifetimes. Lifetime distributions, plotted as survivor plots, for gA⁻(13) channels (Top) and AgA(15) channels (Bottom). The shorter gA⁻(13) channels have lifetimes that are 10-fold less than those of the longer AgA(15) channels. Each histogram is fit by single exponential distributions. Dashed lines denote fits of single exponential distribution to the results. The average lifetimes from the curve fits are 13.4 ± 0.1 ms, 17.0 ± 0.1 ms and 19.5 ± 0.1 ms for the gA⁻(13) channels and 152.6 ± 0.6 ms, 198.3 ± 1.0 ms and 260.0 ± 1.4 ms for the AgA(15) channels. 1.0 M NaCl, pH 7.0; 25 °C; 200 mV; 500 Hz.

Figure 10: Effect of BDM on lifetimes of channels of different length and chirality. To compare the results for different channel types, AgA(15) (►), AgA⁻(15) (◄) and gA⁻(13) (■), the results for each channel were normalized relative to the lifetime in the absence of BDM (τ_{ctrl}) and plotted as mean $\pm$ SD ($n \geq 3$). The control lifetimes, in the absence of BDM were: 14.1 ± 1.4 ms for the gA⁻(13) channels; 162 ± 24 ms for the AgA(15) channels; and 149 ± 14 ms for the AgA⁻(15) channels. 1.0 M NaCl, pH 7.0; 25 °C; 200 mV; 500 Hz.

Figure 11: Effect of BDM on the gramicidin channel appearance rates. Top: normalized appearance rates for AgA(15) (►) and gA⁻(13) (■) channels. The data are plotted as the geometric mean $\pm$ SD ($n \geq 3$) of the ratio of the channel appearance rates measured just before (f_{ctrl}) and $10 - 20$ min after the addition of either 10 or 20 mM BDM. Bottom: the relative changes in the appearance rate of gA⁻(13) channels (vs. AgA(15) channels). The data are based on the relative changes in gA⁻(13) channel and AgA(15) channel appearance rates in the

individual experiments, and are plotted as mean $\pm$ SD ($n \geq 3$). 1.0 M NaCl, pH 7.0; 25 °C; 200 mV; 500 Hz.

Figure 12: Effect of BDM on the time-averaged channel concentrations and free energy of gramicidin channel dimerization. Left ordinate, relative changes in the time-averaged channel concentrations ($f{\cdot}\tau_{)}/f_{cntrl}{\cdot}\tau_{cntrl}$) for the AgA(15) (▶) and gA⁻(13) (■) channels. Right ordinate, the changes in free energy (note the sign convention). 1.0 M NaCl, pH 7.0; 25 °C; 200 mV; 500 Hz.

TABLE I

Examples of membrane proteins affected by BDM

membrane protein	effect	phosphorylation	$K_{0.5}$	Gen**	Caps
L- type Ca channels	inhibition	some influence	~ 6 mM [a]	yes [l]	yes [w]
N- type Ca channels	inhibition	some influence	~15 mM [b]	yes [m]	yes [w]
V-dep. Na channels	inhibition	independent	~ 20 mM [c]	yes [n]	yes [x]
V-dep. K channels	inhibition	independent	11-30 mM [d]	yes [o]	yes [y]
V-sensor hair cells	shift $V_{1/2}$	independent	~ 5 mM [e]	NR	NR
GAP junction	inhibition	some influence	~10 mM [f]	NR	NR
ryanodine receptors	activ./inhib.	independent	~ 2.5 mM [g]	yes [p]	yes [z]
K-ATP channels	inhibition	independent	~ 11 mM [h]	yes [q]	NR
Na/Ca exchanger	inhibition	independent	~ 2 mM [i]	yes [r]	NR
Complex I	inhibition	independent	~ 5 mM [j]	yes [s]	yes [aa]
glycine receptor	inhibition	some influence	~15 mM [k]	yes [t]	NR
CFTR	activation	independent	2-20 mM [tw]	yes [u]	yes [bb]
	inhibition	dependent	< 20 mM [tw]		
gramicidin channels	activity increase [tw]	independent		yes [v]	yes [x]

Thirteen different membrane proteins whose function is affected by BDM. The columns indicate the type of effect observed (**effect**), its dependence on phosphorylation (**phosphorylation**), the [BDM] producing half maximal effect (**$K_{0.5}$**), and whether similar effects have been reported for genistein (**Gen**) and capsaicin (**Caps**). NR = not reported to the best of our knowledge.
Footnotes: ** some effects of genistein may have been interpreted as related to tyrosine phosphorylation; [a] Chapman, 1993; [b] Allen et al, 1998; Sada et al (1995) *Arch Int Pharmacodyn Ther* 330:319-31; [d] Lopatin and Nichols, 1993; [e] Frolenkov et al (2001) *J Physiol* 531:667-76; [f] Verrechia and Herve (1997) *Am J Physiol* 272:C875-85; [g] Tripathy et al (1999); [h] Smith et al (1994). *Br J Pharmacol* 112:143-9; [i] Watanabe et al (2001); [j] Scadutto et al (2000) *Am J Physiol*

279:H1839-48; [k] Ye and McArdle, 1996; [l] Ji et al (2004) Sheng Li Xue Bao. 56:466-70; [m] Morikawa et al (1998) *Pflugers Arch* 436:127-32; [n] Balevych et al (2002) *Mol. Pharmacol.* 62:554-65; [o] Washizuka et al (1997) *Heart Vessels*. Suppl 12:173-4; [p] Liew et al (2004). *Biphys J* 86:111A (abstr.); [q] Ogata et al (1997) *Br J Pharmacol*. 122:1395-404; [r] Wang et al. (1997). *Biochem Biophys Res Commun*. 233: 86–90. [s] Salvi et al (2002) *Biochim Biophys Acta* 1556:187-96; [t] Zhu et al (2003) Neuropharmacology 45:270-80; [u] Weinreich et al, 1997; [v] Hwang et al, 2003; [w] Hagenacker et al (2005) *Brain Res* 1062:74-85; [x] Lundbæk et al, 2005; [y] Park et al (2003) *Brain Res*. 962:135-43; [z] Eun et al (2001) *Biochem Biophys Res Commun* 285:1114-20; [aa] Dedov et al (2001) *Neuroscience* 103:219-26; [bb] Ai et al, 2004; [tw] this work.

$$2M \overset{k_1}{\underset{k_{-1}}{}} D$$

d_0 l

Compression

Bending

Fig. 1

Fig. 2

FSK   FSK   FSK   FSK

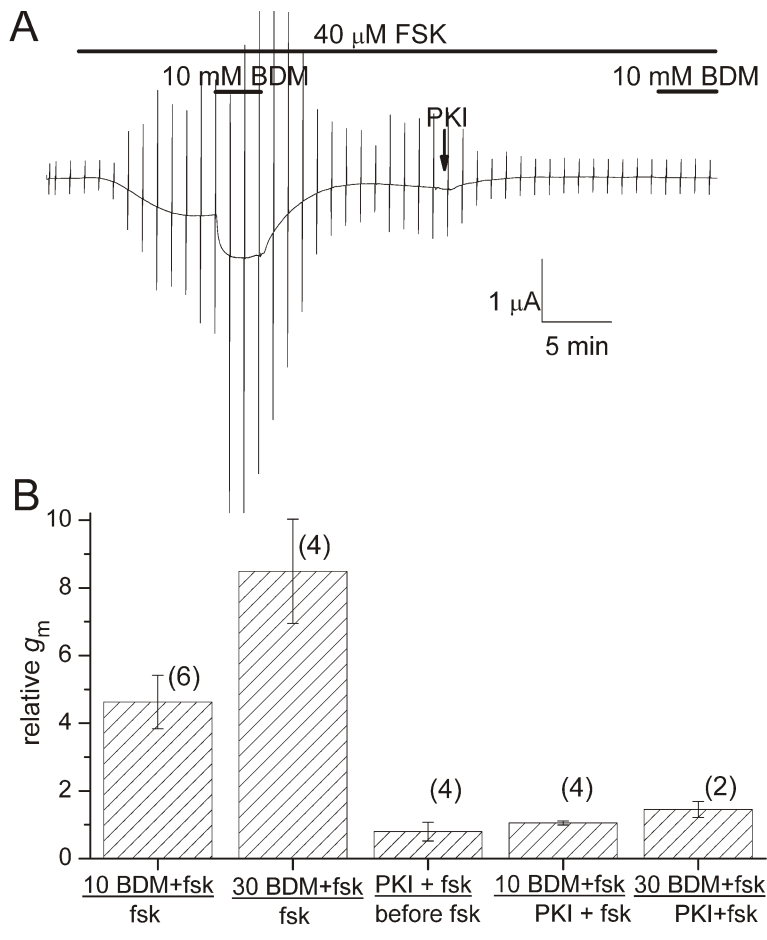   BDM   BDM

                                    microcystin

200 pA

5 min

Fig. 3

Fig. 4

Fig. 5
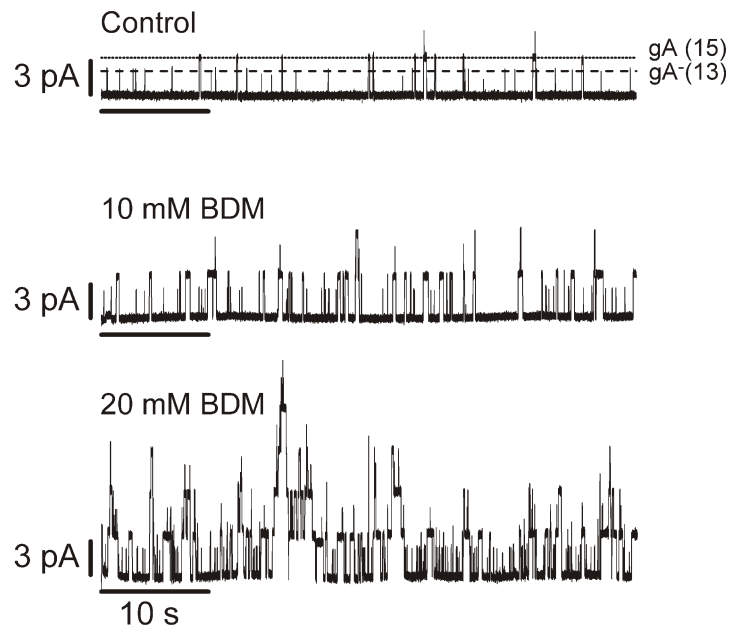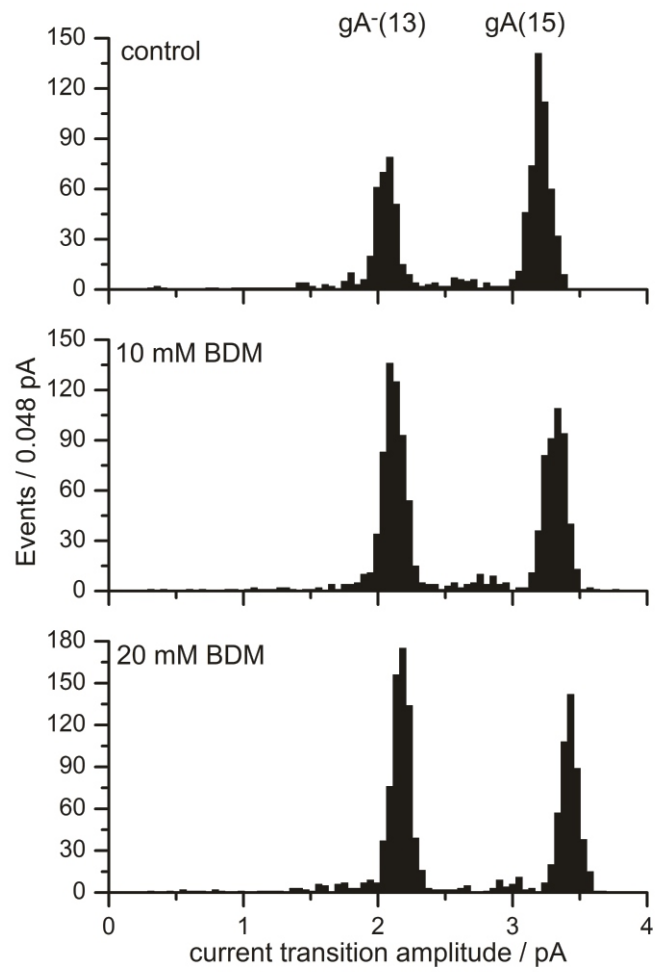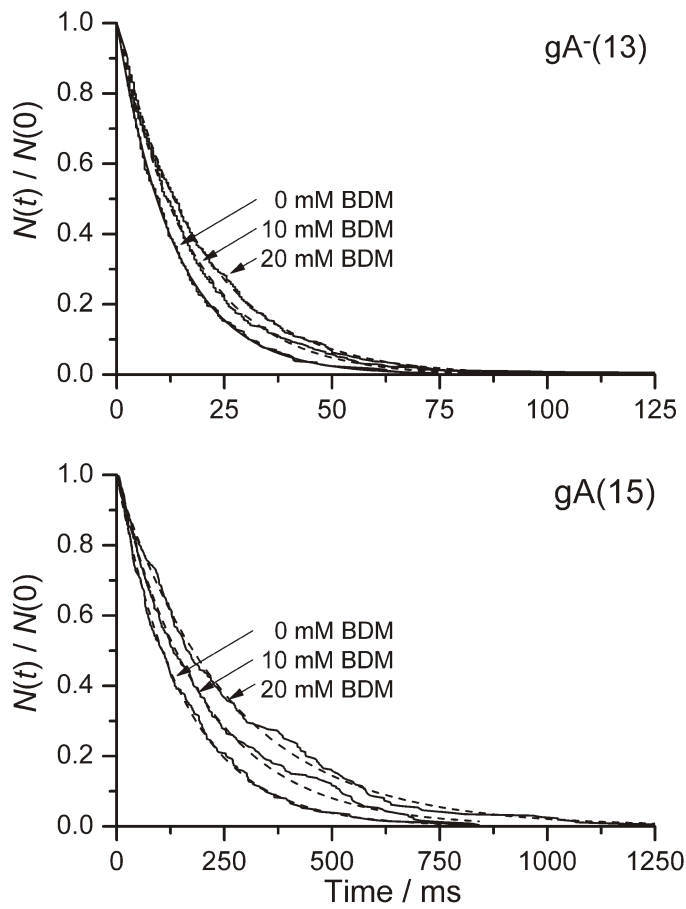
Fig. 6

Control

3 pA

gA (15)
gA⁻(13)

10 mM BDM

3 pA

20 mM BDM

3 pA

10 s
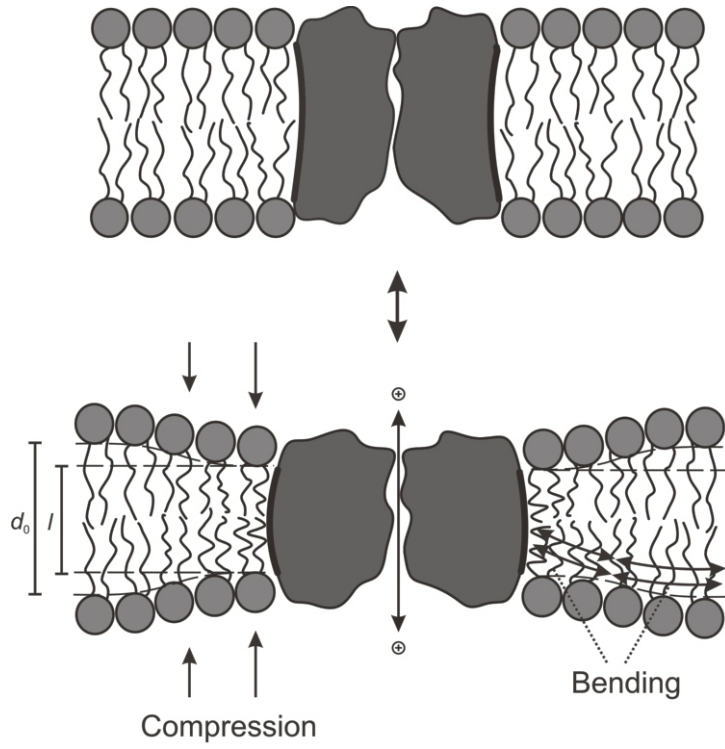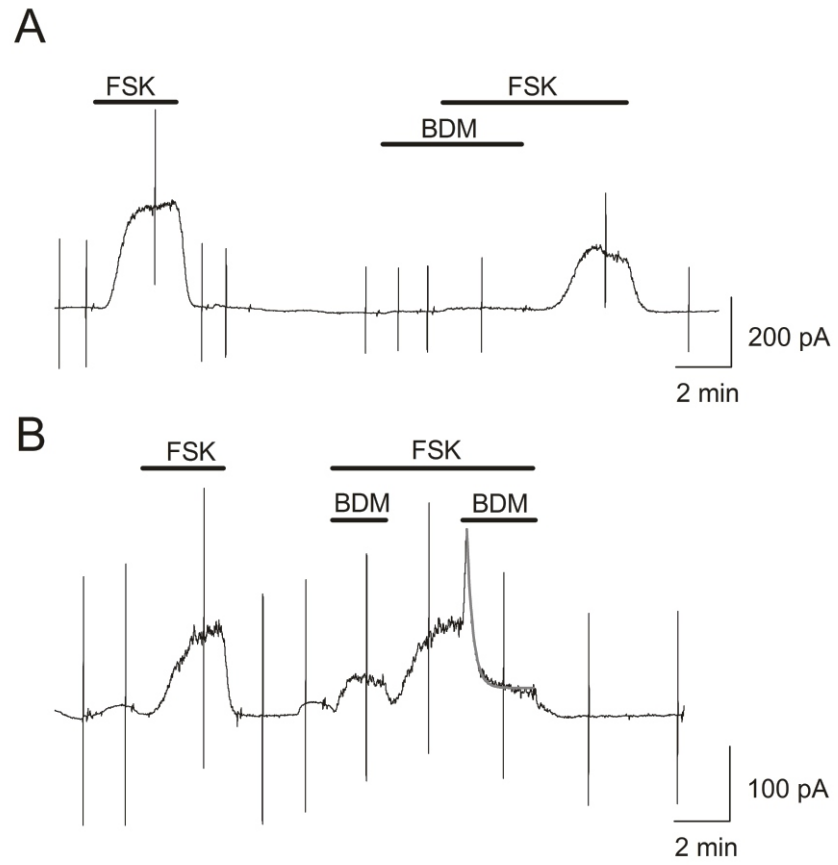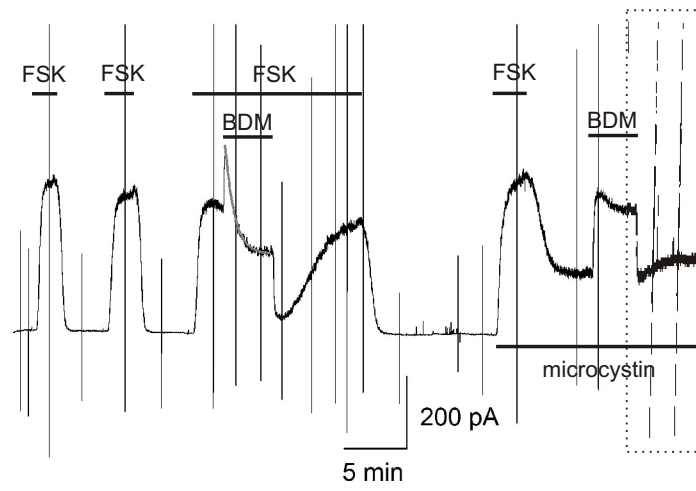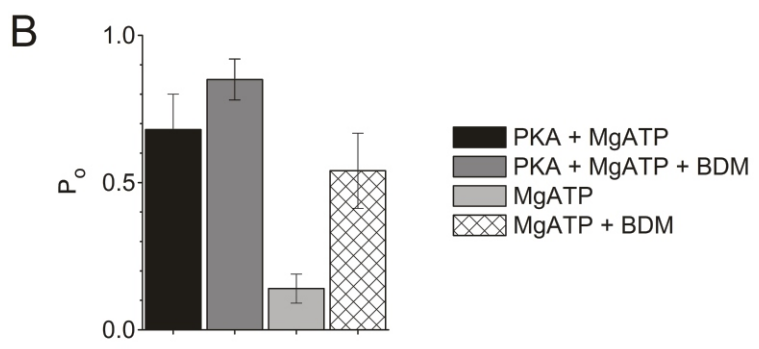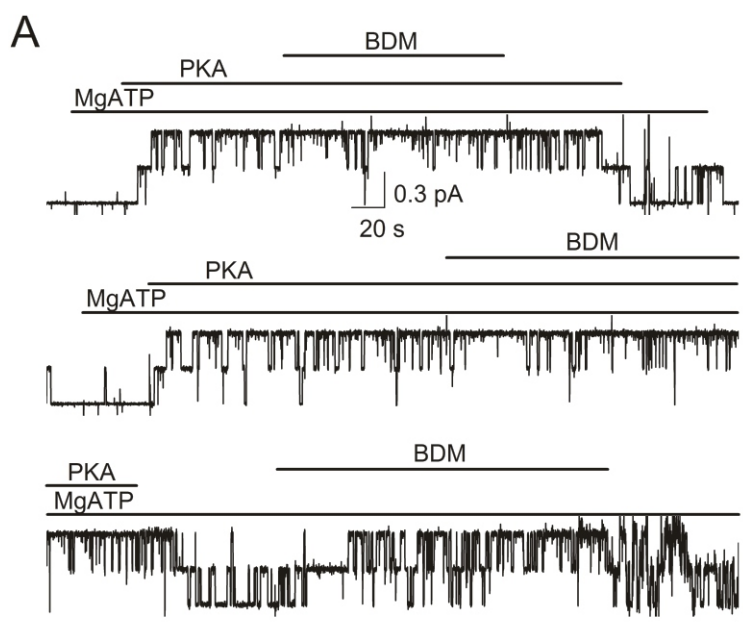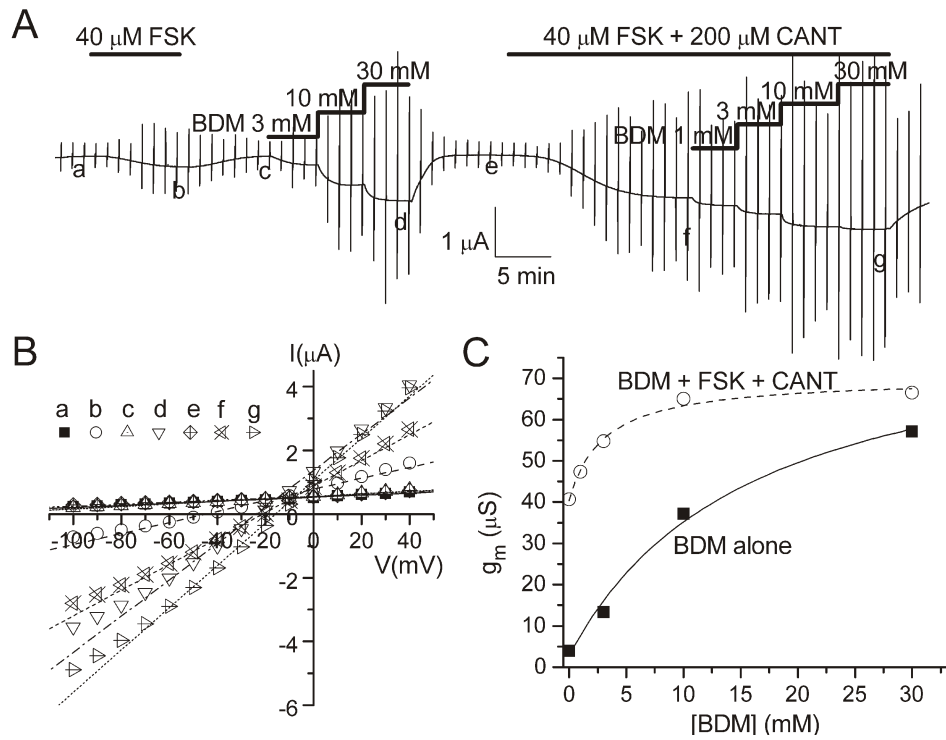
Fig. 7

Fig. 8

Fig. 9

Fig. 10

Fig. 11

Fig. 12